LOW ENERGY BEAM DIAGNOSTICS AT THE VENUS ECR ION SOURCE*

D.S. Todd#, D. Leitner, and M. Strohmeier, LBNL, Berkeley, CA 94720, U.S.A.

Abstract

A dedicated effort to accurately simulate beam extraction and transport from the superconducting electron cyclotron resonance (ECR) ion source VENUS (Versatile ECR for NUclear Science) using particle-in-cell methods has been underway at Lawrence Berkeley National Laboratory (LBNL). The wide range of beam diagnostics used along the VENUS transport system has been essential in benchmarking simulation against experiment. Measurements with some of these devices are presented and are compared with simulation.

INTRODUCTION

The fully-superconducting electron cyclotron resonance (ECR) ion source VENUS at LBNL serves as the prototype injector for the future radioactive ion beam accelerator in the United States [1]. Additionally, a dedicated effort at LBNL has been underway to develop a highly-adaptable, particle-in-cell simulation code to serve as a design tool for future sources and accelerators [2]. Benchmarking simulations against experiment plays a crucial role in model development, and for this reason the transport system for the VENUS ion source has been outfitted with a wide range of diagnostic devices.

Plasma confinement in an ECR ion source is provided through the superposition of solenoidal and sextupolar magnetic fields. Solenoids at each end of the source and a surrounding sextupole produce a confining magnetic field whose magnitude increases in all directions from the source center. This source-centered minimum is surrounded by a series of closed surfaces of constant magnetic field magnitude, and by supplying microwave heating at a frequency matching the electron cyclotron frequency on one or more of these surfaces electrons can be resonantly heated to produce and maintain a plasma through step-wise ionization.

Though the field geometry in ECR ion sources has proven very effective for producing high-current, multiple-charged ion beams, there are inherent characteristics of these sources which make difficult both analysis and simulation of extracted beams including:

- Superposed magnetic field confinement produces asymmetric plasma distributions at extraction
- Plasma is maintained through step-wise ionization, therefore extracted heavy ion beams are typically composed of thirty or more ion species
- Positional distribution of different ion species at the plasma extracting face is unknown
- Beams are extracted at a peak solenoidal magnetic field of up to 3 tesla which falls to zero over the first half-meter of travel giving each extracted ion species a different dynamical behavior
- Beam space charge self fields must be taken into account

From the outset, beam diagnostics have played an important role in the improvement of VENUS ion beam models. As an example, initial simulations of ion distributions at the plasma aperture indicated that while the plasma distribution had a triangular cross section, as expected, this distribution was much larger than the 8-mm diameter beam extraction aperture, was homogenously filled, and should have resulted in an axially-symmetric extracted beam. However, as can be seen in figure 1, imaging of a single species ion beam (He^+) on a 0.25-mm thick tantalum sheet just after extraction shows a triangular cross-section, making it clear that the initial conditions used for the simulation were invalid. As the initial ion beam distribution at the source extraction aperture is unknown and cannot be directly measured or computed, we are using various ion beam diagnostics to refine our simulation model as described in the following sections.

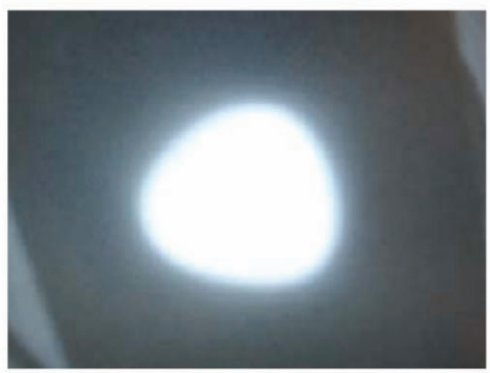

Figure 1: Beam imaging of a He^+ beam with the tantalum sheet, left, shows triangular beam structure 80 cm after extraction.

PARTICLE-IN-CELL SIMULATION OF VENUS EXTRACTION AND TRANSPORT

The layout of VENUS and its accompanying beam transport system are shown in figure 2. Beams are extracted across potentials of up to 30 kV, and the shape of the extracting surface of the plasma can be optimized by a movable accel-decel extraction system. A solenoid lens and a mass analyzing dipole magnet serve as the only two optical elements after the source when used for ion

* Work supported by the Director, Office of Energy Research, Office of High Energy & Nuclear Physics, Nuclear Physics Division of the U.S. Department of Energy under Contract DE AC03-76SF00098
#dstodd@lbl.gov

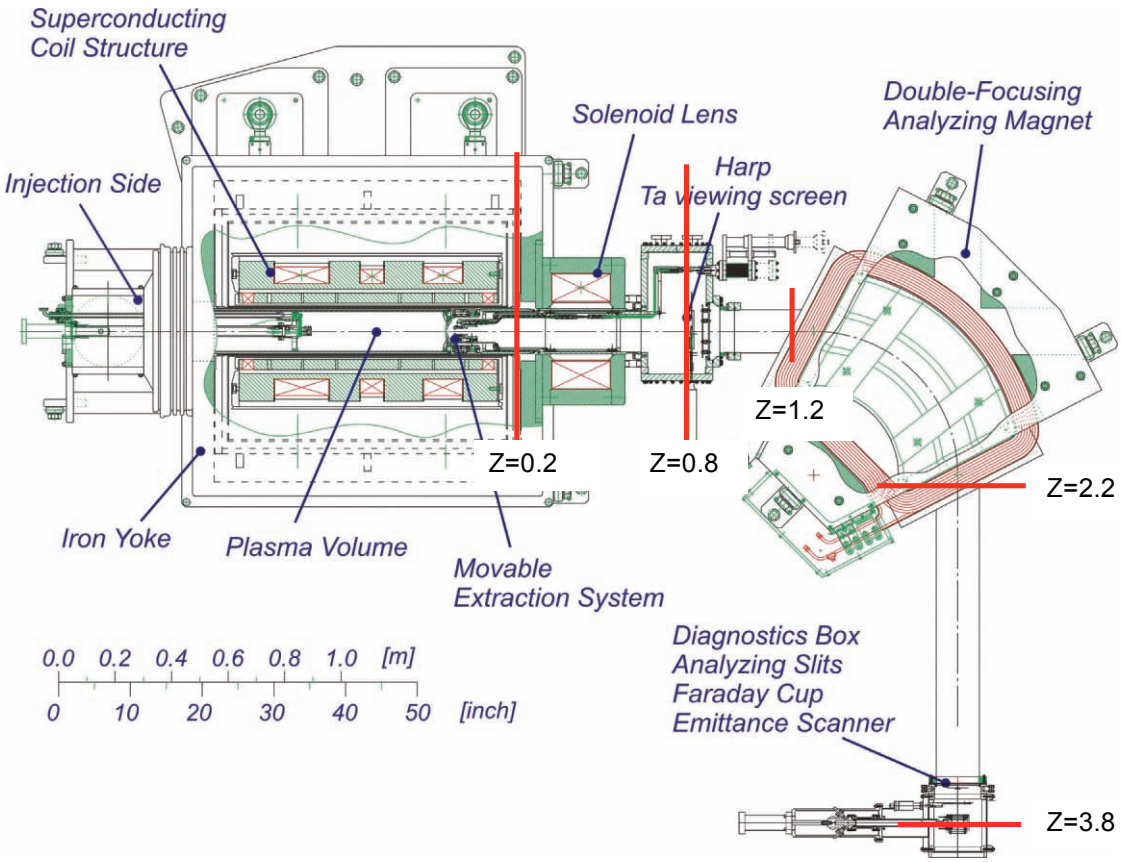

Figure 2: VENUS ion source and transport system layout viewed from above. The indicated lines indicate points at which beam profile measurements will be compared with simulation in the following sections.

beam analysis. The result of this layout is that there are two primary diagnostic regions for the VENUS system: the first is located between the solenoid lens and the analyzing dipole, and the second is located after the analyzing dipole. As the first region is located before the dipole, all ion species are present in the beam complicating analysis greatly. After the dipole magnet analysis is simplified by the presence of only one ion species, but the strong beam asymmetries introduced to this ion species by those charge states over- or under-bent in passing through the dipole complicate the post-dipole beam as well.

Particle-in-cell (PIC) modeling was chosen as the method of simulation for the VENUS system as PIC codes are capable of accurately simulating systems made up of multiple types of interacting particles [3]. The three-dimensional PIC code WARP is well-tested in beam transport modeling and capable of simulating beam transport including both external and self electromagnetic fields [4]. We have enhanced this code by adding a three-dimensional plasma extraction model to allow for the simulation of multiple-species ion beams from asymmetric plasma sheaths. With the addition of this extraction model it is now possible to use WARP to simulate the entire transport system including the plasma extraction in one self-contained code.

For simulations of the VENUS transport system the cross section of the plasma at extraction has been set using field line tracing from experimentally-measured, highly-localized plasma ion sputter marks on the source chamber surface [2]. This method assumes that the ions sputtering the chamber are representative of the ion distribution throughout the source along field lines. In other words, scattering between the plasma and chamber walls doesn't largely affect the measured distribution and it can be as an indicator of the distribution within the plasma. This method of tracking field lines from sputter marks has the distinct advantage that it leads to a triangular ion distribution at the extraction plane that is smaller than the aperture based on measurable properties. The simulations shown in figure 3 are cross sections at the four locations along the transport system indicated in figure 1 for a multi-species and multiple charge state oxygen beam (primarily oxygen with hydrogen and carbon impurities) where a constant triangular distribution based on the plasma sputter marks has been assumed for all ion species.

BEAM DIAGNOSTICS

Viewing screens before dipole

The tantalum viewing screen discussed in the introduction is very useful for imaging single species ion beams of sufficient current to heat the tantalum to glowing. However, for multi-species beams the rotation of the various ion species upon extraction blurs out the

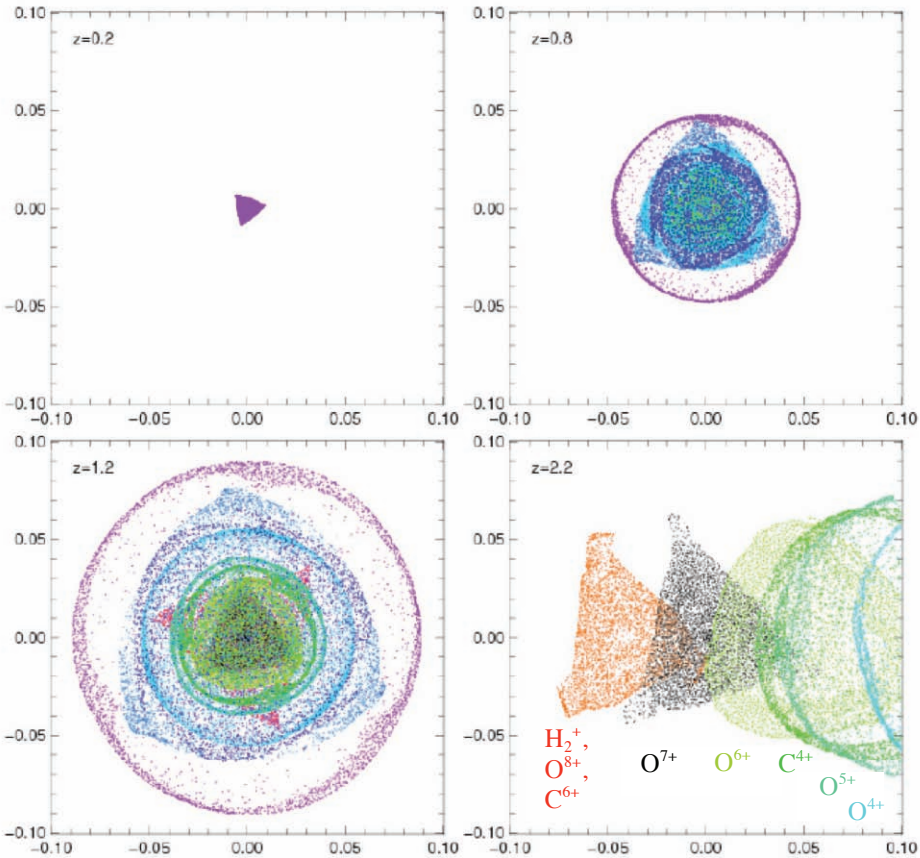

Figure 3: Simulated beam cross sections are plotted for a multi-charge state oxygen beam at four locations along the VENUS transport system: 0.2, 0.8, 1.2, and 2.2 m after the extraction aperture from left to right, top to bottom, respectively). Different colors represent different oxygen charge states and the axes are of meter scale. The development of hollow beams for some species can be seen beginning at 0.8 m, and beam separation immediately after the magnet is clear at 2.2 m.

triangular structure using this method. Therefore, in addition to the tantalum we have used quartz viewing screens that can be inserted into the beam line both before and after the analyzing dipole. As can be seen in figure 4 where the quartz was inserted at 0.8 m after extraction, the triangular structure for multiple ion species is visible for the imaged oxygen beam. In particular, figure 4 should be compared to the simulation shown in figure 3 at 0.8 m.

Beam profile measurement (harp)

Quantitative current density distribution measurements before the analyzing dipole are performed with a harp scanner composed of 62, 0.1-mm diameter wires contained in a 5.0 cm square window, with half of the wires running in parallel to the vertical and half parallel to the horizontal directions.

To investigate beam asymmetry from the VENUS source we extracted single component, He^+ beams in two modes: normal operation and an operational mode with the confining sextupole magnets turned off. In turning off the sextupole the resulting plasma is axially symmetric (axial mirror field only), however this mode is not used for typical operation as the plasma confinement, and hence performance, is greatly reduced.

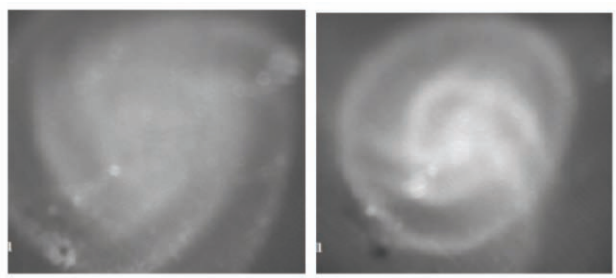

Figure 4: Beam imaging of an oxygen beam using the quartz viewing screen 80 cm after extraction for two solenoid lens current settings: 400 A, left and 500 A, right. Multiple ion species are visible as rings and triangular structure which rotate and focus with increased lens current.

Figure 5 shows measurements with the harp of the beam cross section in the vertical and horizontal

directions when producing a He^+ beam with the sextupoles off for two settings of the solenoid lens. As can be seen in this figure, the measured beam is symmetric and decreases in width as the solenoid lens current is increased (beam is focused).

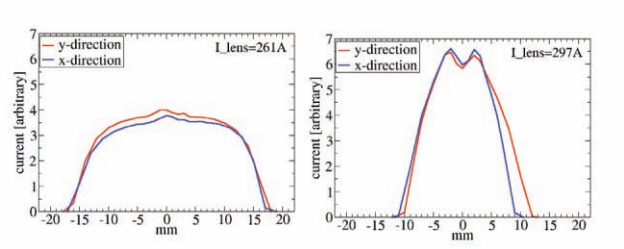

Figure 5: He^+ current density profile measurements in the horizontal and vertical directions using the harp for two solenoid lens currents when the source is operated without the sexutpole resulting in an axially symmetric beam. The small tip in the middle of the profile is believed to be the overfocused, low-current He^{2+} component of the beam.

Energizing the source sextupole produces the measurable beam asymmetry of a triangular beam which rotates and shrinks with increasing focusing strengths of the solenoid lens. Figure 6 shows the measured horizontal profile with the sextupoles on for two solenoid settings along with simulation of the same beam. Reasonable agreement between experiment and simulation were achieved at this location.

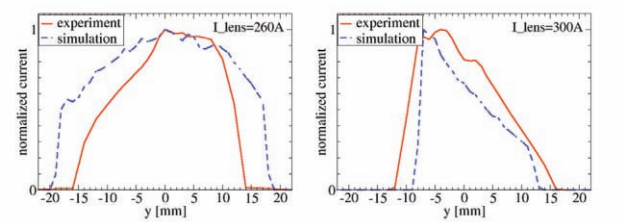

Figure 6: Simulated He^+ current density profiles, dashed, compared with experimental measurement at the harp, solid, for two solenoid lens current settings

Degree of neutralization

Ionization of background gas by the passing beam produces both low energy electrons and ions inside of the beam envelope. These new electrons can be confined by, and effectively reduce, the beam's positive potential, while the newly created ions are ejected from the beam because of the beam potential. We have designed and constructed two retarding potential analyzers, shown in figure 7, to measure the kinetic energy of the ejected ions by measuring the stopping potential distribution for these ions. The devices have three meshes and an electrically isolated plate which is used to measure the ion current. The mesh nearest the beam is at the beam line potential (ground), the voltage of the second is varied to measure the stopping potential of the ions, and the third and closest to the measuring plate is biased negatively to prevent secondary electrons created by ion impact from leaving the measuring plate.

Using an early prototype version of this device at normal operating pressures (~10^{-8} torr) preliminary data showed that stopping potentials were near those one would expect for a beam with no electrons screening the beam space charge, and that the stopping potential decreases significantly as the pressure is raised, as can be seen in the curves plotted in figure 7. This result indicates that although the beam is operated for up to weeks at a time in CW mode (allowing for electron buildup in the beam), the loss rate of confined electrons must exceed the rate of their trapping. However, these surprising results need to be confirmed with the higher resolution energy analyzers.

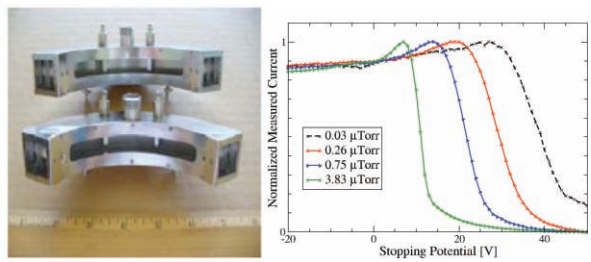

Figure 7: Retarding potential analyzers, left. Measurements of the measured ion current as a function of stopping potential are plotted at right.

Imaging of mass analyzed beams

After the dipole only one species is present, therefore beam analysis is made much simpler. Using a quartz viewing screen mounted at the end of the transport system individual ion species from multiple species beams are imaged. Figure 8 shows an O^{7+} beam imaged on the quartz viewing screen located at z=3.8 m along with the same beam from simulation.

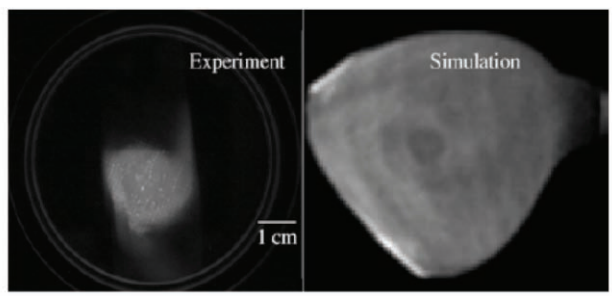

Figure 8: Experimentally imaged O^{7+} beam, left, and the simulated current density plot, right, on the same scale.

As can be seen in figure 8, the general shape of the O^{7+} is reproduced in simulation after passing through the analyzing magnet, but the beam sizes are not in agreement. Imaging and simulation of a C^{4+} from the same extracted beam are shown in figure 9, and once again there is a mismatch in size although the hollowing feature present in the experimental beam is also seen in simulation. Further investigations are needed to determine the source of this discrepancy.

Emittance measurement of mass analyzed beams

In this location quantitative phase space measurements are taken using a pair of Allison-type emittance scanners [5], one aligned horizontally and one vertically to measure x-x' and y-y' distributions. With these devices it has been found that the measured emittance decreases with charge state, whereas analysis of expected emittance growth due to beam extraction in a magnetic field would increase with charge state [1]. This reduced emittance with charge state could be due to smaller initial distributions for highly charged ions at extraction. Alternatively, the hollowing that has been found to occur for low charge state beams [2,6] would decrease emittance with charge state. This hollowing effect can be seen in the simulations in figure 2 at z=2.2 m, where the lower charge state beams, moving right, have hollow distributions while the higher charge state beams, moving left, are closer to constant density.

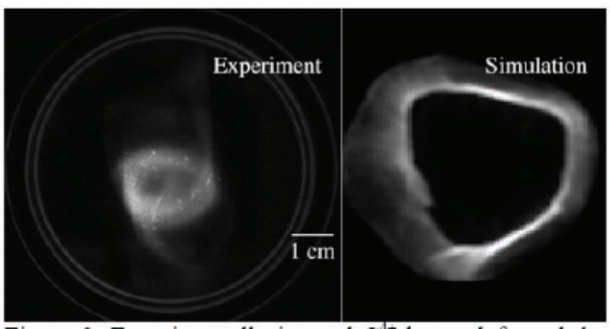

Figure 9: Experimentally imaged C^{4+} beam, left, and the simulated current density plot, right, on the same scale.

Pepper pot---under development

Pepper pot emittance measurement systems have long been in use allowing for the simultaneous measurement of both x' and y' distributions for each hole of the utilized mask [7]. By measuring these distributions over a number of different holes it is possible to obtain a full four-dimensional phase space current density distribution of an ion beam, $f(x_i,y_j,x',y')$, whereas our slit scanners cannot measure transverse correlations. Having this capability is especially important for ECR sources for phase space measurement of measured hollow beam structure, as this hollow structure is much more difficult to extract without cross-correlated phase space information (x-y, x-y', or y-x').

To add this diagnostic capability, a pepper pot system for the VENUS beam line composed of a hole mask, fluorescing material, and CCD camera is under development. We are currently testing hole mask sizes and shapes as well as necessary distances between the mask and the fluorescing material. We have tested three fluorescing materials (quartz plates, Ba_2F, and KBr crystals) and have found the KBr crystals to have the best light response. A measured O^{4+} beam incident on a KBr crytal with a test hole mask is shown in figure 10 along with an analyzed spot showing measured spot structure.

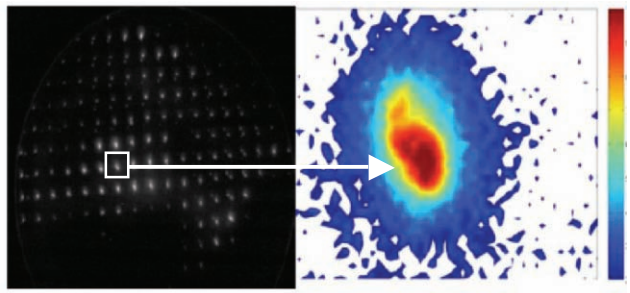

Figure 10: Pepper pot test image of O^{4+} beam, left, with a beam spot's analyzed brightness distribution, right.

FUTURE MEASUREMENT AND SIMULATION

Using the diagnostics we have at present we have found qualitative agreement between experiment and simulation for beam analysis both before and after the dipole with overall shapes and features found experimentally appearing in simulation. However, there are clearly disagreements with regards to properties such as beam size. One free parameter in simulation that needs to be investigated is the level of beam potential screening along the beam line. In simulations to date we have assumed zero beam neutralization as measurements with the retarding potential analyzer have indicated stopping similar to those expected analytically for a nonneutralized beam. However, this analytical check has been done using the approximation of a round beam with a total effective current related to the total extracted current. With the three dimensional extraction simulations it is possible to get a better approximation for the potential at the beam center (and hence necessary stopping potential) for a nonneutralized beam and adjust the level of neutralization accordingly.

Additional simulation improvement will come with the installation of the finalized pepper pot design. Use of this device before the dipole with a simple beam such as He^+ will allow a better understanding of initial conditions while after the dipole it will yield more complete distribution information to investigate beam hollowing.

REFERENCES

[1] D. Leitner, C.M. Lyneis, S.R. Abbott, Nucl. Inst. Meth. B **235**, (2005) 486.
[2] D.S. Todd, D. Leitner, C.M. Lyneis, and D.P Grote, Rev. Sci. Instrum. **79**, 02A316 (2008).
[3] C.K. Birdsall, IEEE Trans. Plas. Sci. **19**, 65 (1991).
[4] Alex Friedman, David P. Grote, and Irving Haber, Phys. Fluids B **4**, 2203 (1992).
[5] D. Wutte, M.A. Leitner, C.M. Lyneis, Physica Scripta **T92**, (2001) 247.
[6] G. Machicoane, et. al., Rev. Sci. Instrum. **79**, 02B714 (2008).
[7] L.E. Collins and P.T. Stroud, Nucl. Instrum. Meth. **26**, (1964) 157.